Epilepsy & Behavior 101 (2019) 106519

Contents lists available at ScienceDirect

Epilepsy & Behavior

journal homepage: www.elsevier.com/locate/yebeh

# Source localization of high-frequency activity in tripolar electroencephalography of patients with epilepsy

Christopher Toole [a], Iris E. Martinez-Juárez [b], John N. Gaitanis [c], Sridhar Sunderam [d], Lei Ding [e], John DiCecco [a,f], Walter G. Besio [a,f,*]

[a] Interdisciplinary Neuroscience Program, University of Rhode Island, Kingston, RI, USA
[b] Epilepsy Clinic and Clinical Epileptology Fellowship, National Autonomous University of Mexico and Mexico's National Institute of Neurology and Neurosurgery MVS, Mexico City, Mexico
[c] Rhode Island Hospital, Providence, RI, USA
[d] Department of Biomedical Engineering, University of Kentucky, Lexington, KY, USA
[e] Stephenson School of Biomedical Engineering, University of Oklahoma, Norman, OK, USA
[f] Department of Electrical, Computer, and Biomedical Engineering, University of Rhode Island, Kingston, RI, USA

ARTICLE INFO

*Article history:*
Received 18 May 2019
Revised 9 August 2019
Accepted 24 August 2019
Available online 6 November 2019

*Keywords:*
Epilepsy
Electroencephalography
High-frequency oscillations
Tripolar concentric ring electrode
Source localization

ABSTRACT

*Objective:* The objective of the study was to localize sources of interictal high-frequency activity (HFA), from tripolar electroencephalography (tEEG), in patient-specific, realistic head models.
*Methods:* Concurrent electroencephalogram (EEG) and tEEG were recorded from nine patients undergoing video-EEG, of which eight had seizures during the recordings and the other had epileptic activity. Patient-specific, realistic boundary element head models were generated from the patient's magnetic resonance images (MRIs). Forward and inverse modeling was performed to localize the HFA to cortical surfaces.
*Results:* In the present study, performed on nine patients with epilepsy, HFA observed in the tEEG was localized to the surface of subject-specific, realistic, cortical models, and found to occur almost exclusively in the seizure onset zone (SOZ)/irritative zone (IZ).
*Significance:* High-frequency oscillations (HFOs) have been studied as precise biomarkers of the SOZ in epilepsy and have resulted in good therapeutic effect in surgical candidates. Knowing where the sources of these highly focal events are located in the brain can help with diagnosis. High-frequency oscillations are not commonly observed in noninvasive EEG recordings, and invasive electrocorticography (ECoG) is usually required to detect them. However, tEEG, i.e., EEG recorded on the scalp with tripolar concentric ring electrodes (TCREs), has been found to detect narrowband HFA from high gamma (approximately 80 Hz) to almost 400 Hz that correlates with SOZ diagnosis. Thus, source localization of HFA in tEEG may help clinicians identify brain regions of the epileptic zone. At the least, the tEEG HFA localization may help determine where to perform intracranial recordings used for precise diagnosis.



## 1. Introduction

Epilepsy affects approximately 70 million people worldwide, making it the second most prevalent neurological disorder [1]. Of all patients with epilepsy, 60% have focal epilepsy syndromes and approximately 15% of these patients have conditions resistant to anticonvulsant drugs. Rosenow and Luders [2] conservatively estimate that approximately 50% of these patients are potential candidates for surgical epilepsy treatment, 4.5% of all patients with epilepsy. In surgery, seizure onset zones (SOZs) or irritative zones (IZs) are removed with good therapeutic effect [3]. The SOZ is defined as the region in which clinical seizures originate while the IZ is the region of cortex that generates interictal epileptiform discharges seen in EEG or magnetoencephalography (MEG) measurements [2]. Thus, EEG potentials play an important role in evaluating suitability for epilepsy surgery [4]. The SOZs and IZs must be correctly identified and localized before surgery [3]. However, conventional EEG has poor sensitivity to localized epileptiform activity [2].

High-frequency oscillations (HFOs) can refer to gamma activity (30–100 Hz), ripples (100–200 Hz), or fast ripples (250–500 Hz) and were first reported in humans by Fisher et al. [5] and Allen et al. [6]. They are high-energy oscillations that have been shown to be a biomarker of epilepsy and highly correlated with the SOZ and IZ [7–9]. Because HFOs arise from synchronous activity of small, focal subsets of neurons,

* Correspondence to: W.G. Besio, Department of Electrical, Computer, and Biomedical Engineering, University of Rhode Island, Kingston, RI, USA.
*E-mail address:* besio@uri.edu (W.G. Besio).

https://doi.org/10.1016/j.yebeh.2019.106519
1525-5050/

intracranial recordings are typically required to detect their localized presentation [10]. High-frequency oscillations have been recorded in the minutes before seizure onset, and the removal of their cortical sources, especially for fast ripples, correlates with positive surgical outcome [5,6,8,11,12]. The sources of fast ripple activity in humans are estimated to be less than 1 $mm^3$ [13]. Thus, microwire electrodes are best suited for their detection. However, Worrell et al. [11] have recently shown that detection of HFOs in this frequency range is possible with clinical macroelectrodes on the scale of 1 to 10 $mm^2$. They utilized hybrid depth electrodes containing both clinical electrocorticography (ECoG) sensors and multiple microwires and found that HFO frequencies recorded with microwires span a continuum from the ripple to the fast ripple range. In contrast, the distribution of HFO frequencies recorded with macroelectrodes falls off more rapidly with frequency, and fast ripples are observed less frequently [11]. Besio et al. [9] have shown that the tripolar concentric ring electrode (TCRE) (Fig. 1) is able to noninvasively record narrowband, high-frequency activity (HFA) in patients with epilepsy. The term HFA is used to differentiate this apparent epileptic activity from previously reported, more wideband HFOs. The increased signal-to-noise ratio and spatial resolution of the TCRE [14,15] make noninvasive measurement of HFA possible in tripolar electroencephalography (tEEG). The novelty of the TCRE design and instrumentation is that two bipolar signals are recorded from three closely spaced, concentric electrode elements. Then, the tripolar Laplacian derivation, first described in Besio et al. [14] is estimated as the weighted sum, $16 * (M - D) - (O - D)$, where O, M, and D are the potentials on the outer ring, middle ring, and central disc of the TCRE, respectively. When compared with conventional EEG signals, tEEG has shown a 6.25-dB increase in signal-to-noise ratio and less than one-tenth (8.27%) the mutual information between a pair of adjacent electrodes [14,15]. Localization of HFA sources by approximation to the nearest electrode(s) [9] has been performed, but more robust methods such as discrete dipole fitting or distributed source methods have yet to be reported with any tEEG signals.

This study aimed to localize HFA in patients with epilepsy to realistic, subject-specific cortical models to determine if HFA sources are correlated with SOZ/IZ clinical diagnosis and could be used as a preliminary indicator of these epileptogenic zones. Consequent identification of SOZs and IZs through tEEG source localization would increase confidence in determining areas for removal in epilepsy surgery. Since these procedures, including invasive EEG (iEEG), are associated with risks to patients including transient and permanent neurologic deficits, infections, hematoma, nonhabitual seizures, cerebral infarction, cerebral edema, and increased intracranial pressure [16,17], it is advantageous to have a better understanding of individual pathology before patients are subject to them.

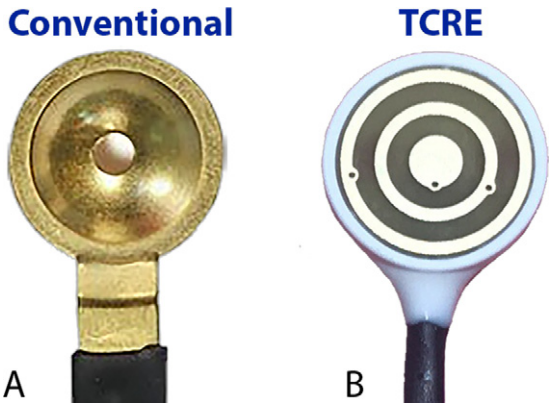


**Fig. 1.** Conventional disc electrode (A) and tripolar concentric ring electrode (B) with a 1-cm diameter.

## 2. Materials and methods

### 2.1. Subjects

Patients A through I were recruited from Rhode Island Hospital (RIH; n = 1; E) and the National Institute of Neurology and Neuroscience (NINN; n = 8) in Mexico City, Mexico after referral by the epilepsy clinic of each institution with the diagnosis of drug-resistant epilepsy, using the International League Against Epilepsy criteria [18]. Epilepsy and epileptic seizure diagnosis was based on the international classification of seizures 1981 [19] and epileptic syndromes 1989 [20]. Recording protocols were approved by each of the institutional review boards. Seizure onset zone diagnosis was performed by an epileptologist at NINN (IEMJ) and RIH (JNG).

### 2.2. Data collection

The tEEG recording protocol was designed to avoid any interference with clinical EEG recording and evaluation. At both the NINN and RIH during the attachment of clinical conventional disc electrodes (referred to as 'EEG electrodes' or 'EEG signals' in the subsequent text), the patient's scalp was cleaned with Nuprep and then, EEG electrodes were affixed to the scalp at the 10–20 International Electrode System locations using Ten-20 paste (and collodion at NINN). To obtain tEEG recordings in parallel to the clinical EEG, the TCREs were placed just behind the disc electrodes in 19 locations close to the 10–10 sites and attached to the scalp with Ten-20 paste (and collodion at NINN) (Fig. 2). The electrical ground was placed on the forehead, and the reference electrode was placed on the forehead at RIH and on the Oz location at NINN. Clinical EEG was recorded with the Comet AS40 system (Grass Technologies, West Warwick, RI) and stored separately for further clinical evaluation. The clinical EEG was digitized at 200 samples per second, and the low-pass filter was 70 Hz. The tEEG data were preamplified with the gain equal to either 6 (n = 5, A–E) or 47 (n = 4, F–I) with a t-Interface 20 (CREmedical, RI, USA) and amplified and digitized with an Aura LTM-64 system (Grass Technologies, West Warwick, RI) at different sampling frequencies for different patients. For two patients (B and C), the data were filtered from 1–100 Hz and digitized at 200 S/s, another one (E) was filtered from 1–200 Hz and digitized at 400 S/s, and for the remaining six patients, the data were filtered from 1–500 Hz and digitized at 1600 S/s. The 60-Hz notch filter was used for all patients. The recording sessions at the NINN usually lasted for six hours, from around 7 am to 1 pm. For the patient at RIH, the recording was stopped shortly after the patient had a seizure (130 min total). The NINN recording protocol included requests that patients be sleep-deprived the night before coming in for video-EEG monitoring and all patients signed an additional consent form as antiepileptic drug dosage was reduced by half the day before the recording. Recorded data were reviewed by the epileptologists, and seizure onset time and duration were determined for each seizure. Seizure onset time was defined as the beginning of the first observable seizure pattern in EEG. Further, it is important to note, the reference location does not appear to have an effect on the TCRE results due to its Laplacian estimation. Moreover, differences in system gain and recording methods are due to development and improvements, spanning several years.

### 2.3. Head modeling

T1-weighted magnetic resonance (MR) images of 7 NINN patients were available for 3-dimensional (3D), subject-specific, realistic head modeling (not E and F). Head models were constructed from these images with the automated procedures of the Freesurfer image analysis suite. Freesurfer is documented and freely available for download online (http://sufer.nmr.mgh.harvard.edu/). In the present study, only a single series of volumetric T1 images was used for each subject. Therefore, motion correction and averaging were not performed. In the Freesurfer

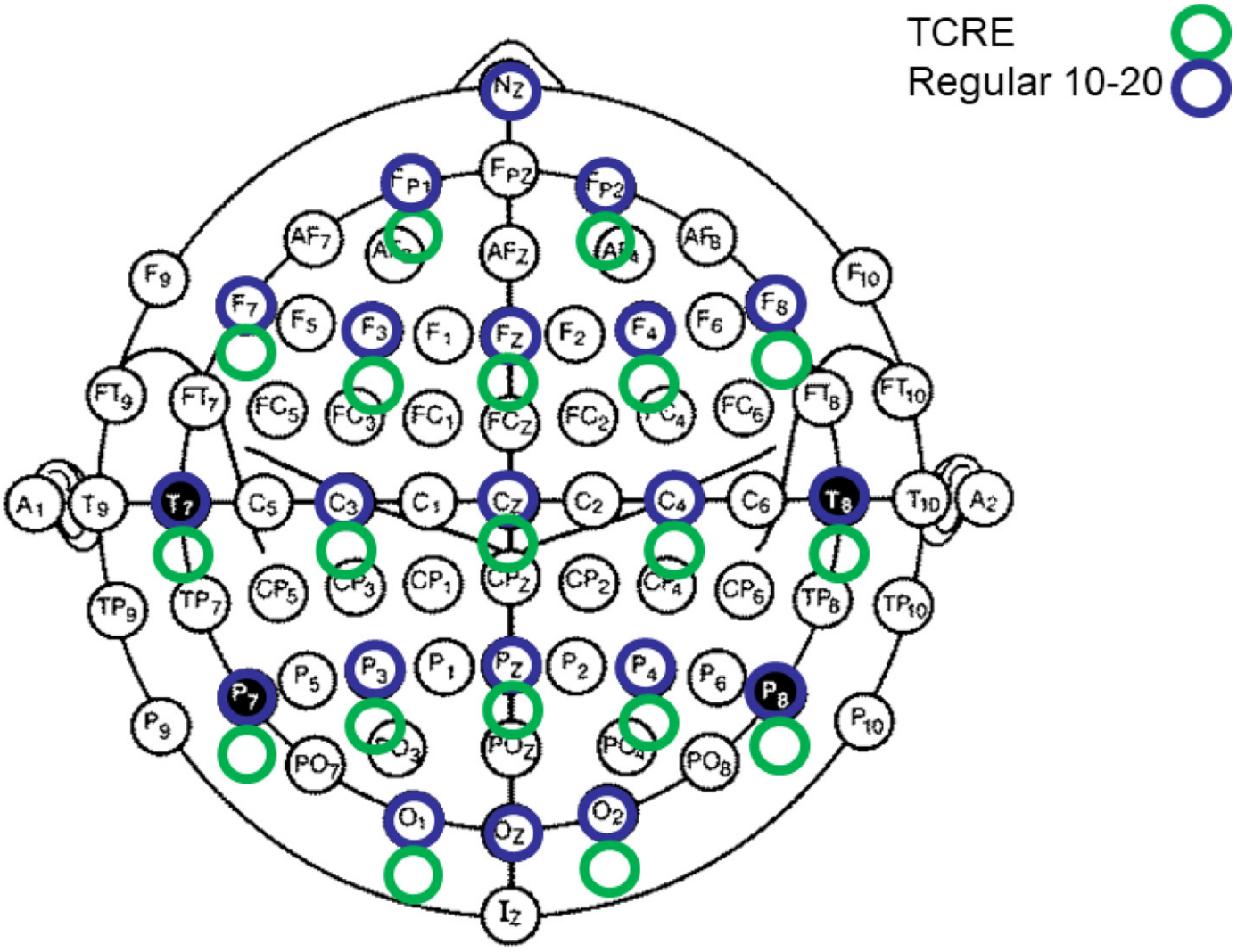


**Fig. 2.** The 10-5 montage with TCREs (green) placed near the 10–20 locations. Note: T7/P7 and T8/P8 are the same as T3/T5 and T4/T6 in 10–20 nomenclature. The blue rings are for standard 10–20 electrode locations.

process, a hybrid watershed/surface deformation procedure [21] is used to remove nonbrain tissue and is followed by an automated Talairach transformation, segmentation of the subcortical white matter and deep gray matter volumetric structures [22], intensity normalization [23], tessellation of the gray matter white matter boundary, automated topology correction [24], and surface deformation following intensity gradients to optimally place the gray/white and gray/cerebrospinal fluid borders at the location where the greatest shift in intensity defines the transition to the other tissue class [25]. Subject models were exported from Freesurfer and imported into Brainstorm for localization analysis. Brainstorm calls OpenMEEG [26] to convert the Freesurfer output into a three-layer boundary element method (BEM) model surrounding the source space of 15,000 dipoles on the cortex surface. These layers include the scalp, skull, and brain with relative conductivity values of 1, 0.0125, and 1, respectively, and each layer consists of 1922 vertices. OpenMEEG then used the BEM to calculate the lead field matrix. Conversion to a tEEG-specific lead field matrix was not performed, as forward model resolution was not sufficient for obtaining differences in potential on the model surface between TCRE rings.

### *2.4. Signal processing and localization*

The data from individual TCRE rings were first preprocessed with the tripolar Laplacian algorithm [14] to obtain the tEEG signal for each electrode. This signal estimates the surface Laplacian by multiplying the difference between the inner ring and center disc by a factor of 16 and then subtracting the outer ring signal. As in Besio et al. [9], a modified version of the algorithm reported by Gardner et al. [27] was used in MATLAB for detection of HFAs and their frequency characteristics. Short-time fast Fourier transform (ST-FFT) power thresholding vs baseline level (mean + 2 standard deviations, per frequency band) was used after band-pass filtering with 55 Hz and 500 Hz cutoffs for HFA detection. High-frequency artifacts such as electrooculogram (EOG) and electromyogram (EMG) were ruled out by visual inspection. Spectrograms were used to analyze the entirety of each recording and identify the most persistent, narrowband HFA in the preictal period. High-frequency activity was deemed persistent if the above threshold requirement was met for at least 33% of a 2-minute, interictal window.

Data were imported into EEGLab (https://sccn.ucsd.edu/eeglab/), a freely available plugin for MAT-LAB. The EEG and tEEG recordings were detrended and notch-filtered (noncausal, zero-phase, IIR Butterworth) to remove direct current (DC) bias and 60 Hz noise, respectively. Then, a noncausal, zero-phase, IIR Butterworth bandpass filter specific to each subject's HFA range was used to isolate the narrowband, high-power activity of each subject. Filters were designed to avoid both loss of gain in the passband and the introduction of ripple artifacts. Data were then imported into Brainstorm [28], which is a freely available (http://neuroimage.usc.edu/brainstorm/) open-source

application for the analysis of MEG, EEG, functional near infrared spectroscopy (fNIRS), ECoG, and other brain recordings.

In Brainstorm, surface potentials of the HFA peaks were localized, on a case-by-case basis, to the surface of cortical models specific to each subject, where available, and the ICBM152 head model was used for patients with no MRI data (E and F). The ICBM152 model is derived from a nonlinear average of magnetic resonance image (MRI) scans of the 152 subjects in the MNI152 database [29]. Only temporally persistent, narrowband HFA were selected for localization. If multiple spatial locations recorded this activity, then each was localized, defined by the peak activity. A whitened and depth-weighted linear L2-minimum norm estimates (MNE) algorithm [30] was used to localize signals to a source space of dipoles constrained normal to the cortical surface of the model, resulting in current density plotted on the model cortical surface. For a full description of this localization method, please refer to Section 6, "The current estimates", of the MNE manual [31], which is available for download (http://www.martinos.org/meg/manuals/MNE-manual-2.7.pdf).

### 2.5. HFA localization and correlation with SOZ/IZ diagnosis

To assess the relationship between the identified HFA sources and the clinical diagnosis, the ratio of patients in which HFA generators fell within the SOZ/IZ over the total number of patients was calculated. The ratio of patients in which HFA was localized to areas outside the SOZ/IZ was also calculated to access the selectivity of HFA as an indicator of SOZ/IZ. The SOZ or IZ was determined for each patient by the epileptologists based on EEG data, video-EEG, patient history, and medical imaging such as MRI and positron emission tomography (PET). These clinicians did not have access to tEEG data and were not aware of the HFA detection and localization results. Both neurologists did not asses all subjects. Each subjects' primary neurologist diagnosis was used for comparison to TCRE HFA localization. In one patient (E), the SOZ was determined by intracranial ictal recordings and seizure cessation following surgical resection.

## 3. Results

### 3.1. HFA detection and localization

Epileptiform HFA was found and localized in the tEEG recordings of nine patients with epilepsy. Eight of these subjects experienced clinical seizures during recording, and T1-weighted MRI data were available for the construction of seven subject-specific head models. The ICBM152 average head model was used for the remaining two subjects (E and F). Localized HFA fell into the high gamma, ripples, and fast ripples range in three subjects each. These findings are summarized in Table 1, which shows the source location of HFA, the frequency of this activity, SOZ/IZ diagnosis, whether or not the source location and diagnosis agree, if additional sources were found outside the diagnosed SOZ/IZ, and the head model (ssm = subject-specific head model) for each subject. Subjects that did not exhibit HFA outside SOZ/IZ also did not have HFA outside of the reported frequency (± approximately 10 Hz). Subjects D (nonfocal onset), E, and I had HFA outside the reported frequency albeit less often, and subjects E and I had shorter duration (transient-like) HFA outside of the SOZ/IZ, also less often.

A representative example of the recorded HFA in patient G is shown in Fig. 3. At the time of recording, this patient was a 62-year-old male with a right frontotemporal lobe SOZ diagnosis. He had been experiencing complex partial seizures (CPS) with a frequency of one per month and was being treated with 500 mg levetiracetam (LEV). An MRI had revealed a left temporal brain tumor and issues with the intensity of the white subcortical and deep matter in the left temporal lobe. The same region exhibited hypometabolism in PET imaging. Fig. 3(a) displays the tEEG time series of a 1-second segment containing HFA at the 238.5-second mark, preceding a CPS by approximately 8 min. High-frequency activity is apparent at locations P3, O1, Pz, and F8. The power spectral density of the same segment of data can be found in Fig. 3(b). A sharp peak is visible at 320 Hz for those four channels but not the others.

Fig. 4 shows the spectrograms for channels P3, O1, Pz, and F8 in panels (a), (b), (c), and (d), respectively. Persistent 320 Hz activity is seen in all four channels. The exact instant shown in Fig. 3 can be seen at approximately the 238-second mark (circled), soon after the first instance of increased power across all frequencies. Peaks of this HFA example were then localized on the cortex surface of the subject-specific model and shown in Fig. 5. Fig. 5(a) contains the localization of moderate HFA generated outside of the SOZ while panels (b)–(d) display stronger HFA localization within the SOZ. Figs. 3–5 display a TCRE HFA as EEG time-series, power spectrum, time-frequency components, and inverse source modeling with the given representative example. This example was chosen for localization (and others not shown) because of its persistence in time during the interictal period, narrow bandwidth (approximately 10 Hz), and its high frequency.

### 3.2. SOZ/IZ correlation

High-frequency activities preceding seizures were localized to the SOZ in eight of the nine patients. No SOZ was determined in the remaining patient, so HFA source map correlation to the IZ was accessed instead. The seizure of this patient (D) was determined to be of nonfocal onset, and widespread HFA sources were observed, so patient D was excluded from accessing the selectivity of HFA sources as indicators of SOZ. The HFA sources of patient D were considered within the SOZ/IZ for correlation calculation. High-frequency activities were localized within the diagnosed SOZ/IZ in all nine of the patients (100%). A focal diagnosis was determined for eight patients. In only three of these patients (37.5%), sources of HFA above noise levels, 2-SD above the mean, were found outside of the SOZ/IZ. Fig. 5(a) is an example of HFA sources found outside the diagnosed SOZ (right frontotemporal region circled in panels (b)–(d)) of patient G.

## 4. Discussion

Electroencephalogram source localization (ESL) is fundamentally broken into the forward and inverse problem when determining

**Table 1**
Summary of HFA localization results.

| Patient | HFA source | Frequency (Hz) | SOZ/IZ | Agree? | Outside? | Head model |
|---|---|---|---|---|---|---|
| A | Left frontotemporal | 120 | Left frontotemporal | Yes | No | ssm |
| B | Left occipital | 75 | Left occipital/parietal | Yes | No | ssm |
| C | Bilateral frontotemporal | 75 | Bilateral frontotemporal | Yes | No | ssm |
| D | Nonfocal | 330 | Nonfocal | Yes | N/A | ssm |
| E | Right motor/frontal, left motor/temp./front/par. | 63 | Left premotor | Yes | Yes | ICBM152 |
| F | Right temporal | 394 | Bilateral temporal | Yes | No | ICBM152 |
| G | Right frontotemporal, left temporal/parietal | 320 | Right frontotemporal | Yes | Yes | ssm |
| H | Right temporal | 110 | Right temporal | Yes | No | ssm |
| I | Left temporal/parietal/occipital | 110 | Left parietotemporal | Yes | Yes | ssm |

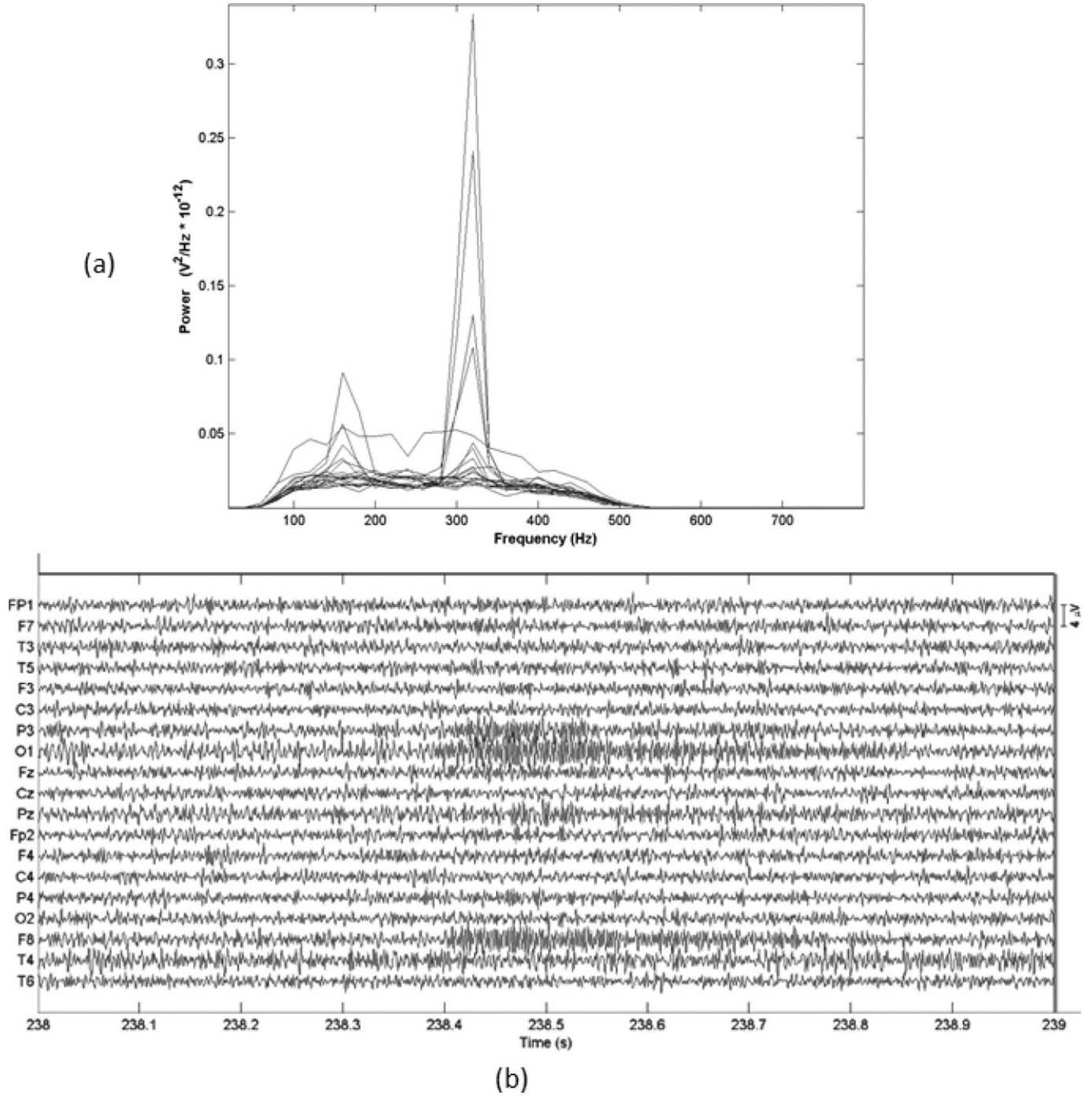


**Fig. 3.** A representative example of the HFA recorded in patient G shown in the time domain (b) and its power spectral density (a). Activity below 55 Hz and above 500 Hz was filtered, forward and backward for zero phase, with a fifth order Butterworth IIR filter. High-frequency activity is most prominent at approximately 238.5 s in TCRE channels P3, O1, Pz, and F8. The four largest peaks at 320 Hz in (a) are of the same four channels.

cortical sources of signals measured on the scalp surface [30,32]. Identification of the source from signal is the inverse problem. The forward problem is the propagation of signals from source to the scalp surface, and its solution, the forward model, is necessary to solve the inverse problem [33]. Specifically, the head model, and its compartments, surfaces, conductivities, and coregistered electrode locations comprise the forward model, also known as the volume conductor [32].

The inverse problem is ill-posed since there are infinite numbers of source configurations that can result in the same potential distribution on the head surface. Therefore, additional constraints to the source space must be used to find a unique solution. The present study utilizes the linear MNE method since it is most commonly used [32], produces good results when localizing distributed networks of brain activity seen in epileptic discharges, and is robust, allowing for statistical analysis and normalization of the cortical source distributions [3,30,34]. Moreover, minimum-norm cortical source estimation is robust against error in the skull conductivity parameter of the forward model that is not a well-known value [35].

The choice of head model is important to finding an accurate solution to the inverse problem. Realistic head models offer increased localization accuracy over simple shell models [36], and subject-specific realistic models have been shown to further increase accuracy in localizing epileptogenic zones in a case study of 152 patients [3]. For this reason, subject-specific, realistic head models were used in the present

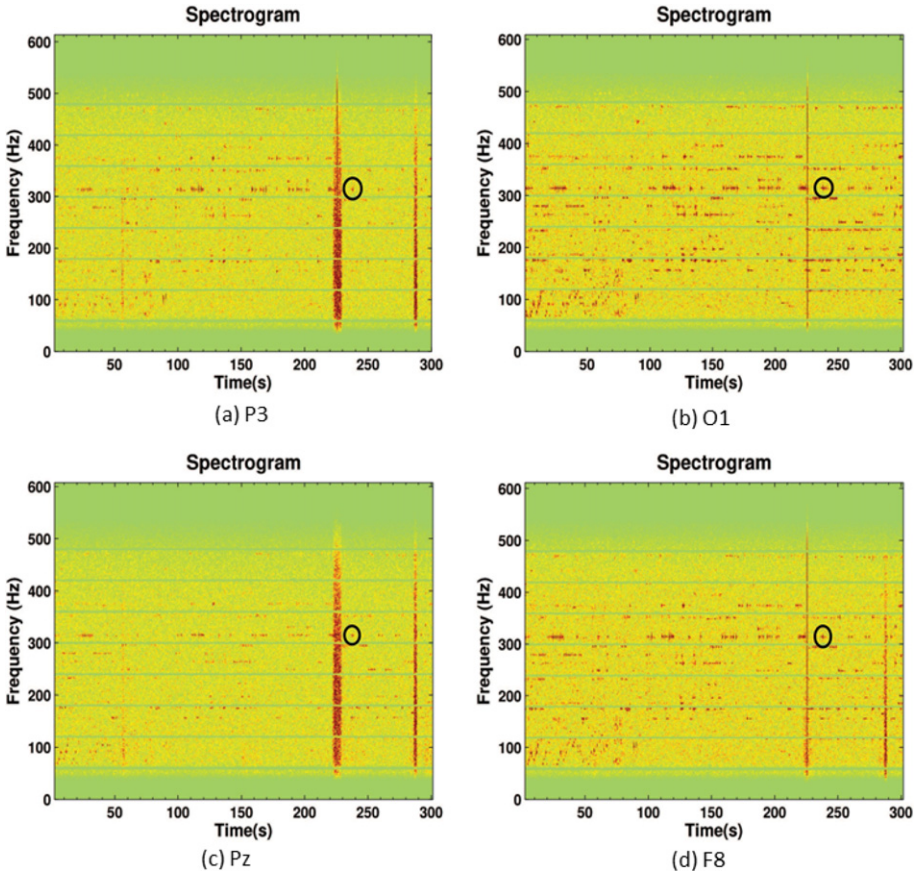


**Fig. 4.** Spectrograms of the HFA signals (circled) shown in Fig. 3, built from short-time Fourier transform with 1 s Hamming windows of 50% overlap. The TCRE channels P3 (A), O1 (B), Pz (C), and F8 (D) are shown. Circled activity is localized in Fig. 5. Activity below 55 Hz and above 500 Hz was filtered, forward and backward for zero phase, with a fifth order Butterworth IIR filter. A 60-Hz notch filter was also applied.

study for HFA localization where individual MRI data were available. In patients for whom these data were not available, a realistic template, head model was used.

Artifacts originating from scalp muscles, eye blinks, eye movements, or patient movement often contaminate EEG recorded with conventional disc electrodes [37], and these artifacts greatly hinder the interpretation of recorded seizures when they occur at the time of seizure onset [38]. To make matters worse, tonic or tonic–clonic seizures are characterized by prominent muscle activity, increasing the effects of these high-frequency artifacts [39]. In a previous study using five of the present nine patients, Besio et al. [9] found that the TCRE automatically attenuates myogenic activity and movement artifacts without the loss of information that is coupled with conventional artifact removal techniques in digital signal processing. This loss is often unavoidable in conventional EEG when EMG artifact is within the same frequency range as high-frequency components of brain activity. It was also shown that high-frequency brain activity was evident in the tEEG where it was undetected in conventional EEG, and its subsequent source estimation by electrode location was highly correlated with the diagnosed SOZ [9].

The present study attempts to extend those findings to a greater number of patients and perform more robust source localization of the HFA. In nine patients with epilepsy, HFA was recorded with tEEG and localized to the surface of realistic, 3D cortical models. High-frequency activity sources were found in the diagnosed SOZ/IZ of all nine patients. Eight of these patients were diagnosed with a focal SOZ based on conventional EEG, and in only three of them, HFA sources were found outside of the diagnosed SOZ. These three patients were E, G, and I in Table 1. As shown in Fig. 5, HFA sources were found in the left temporal and parietal regions of patient G, outside the diagnosed right frontotemporal SOZ. However, functional MRI of this patient revealed a tumor in the left temporal lobe, issues with the intensity of white subcortical and deep matter in the left temporal lobe, and destruction of fibers in the rostral portion of the uncinate fasciculus. In PET imaging, hypometabolism was found in the left temporal lobe, especially in the posterior inferior temporal gyrus. It is possible that these conditions may explain the left hemispheric HFA sources found in this patient. Thus, HFA may prove to be a useful biomarker for other epileptic etiologies in addition to the clinical SOZ. For example, before the pathology of patient D progressed to a generalized, nonfocal seizure onset, HFA was found locally in the left hemisphere. It was later revealed in MRI that this patient suffered from mesial temporal sclerosis in the left temporal lobe. Future studies should explore the validity of HFA found in tEEG as biomarkers for specific etiologies of epilepsy.

The other two patients (E, I) who experienced HFA sources outside of the diagnosed SOZ did not suffer these or other conditions to help explain such results. Sources of the said activity were found in the left temporal and parietal SOZ of patient I in addition to the left occipital lobe. It is probable that the left occipital result is due to the proximity of the region to the SOZ. In the case of patient E, HFA sources were found in the left premotor SOZ as well as the surrounding brain regions and the contralateral hemisphere. Interhemispheric connections between the two motor regions could explain these results.

Other possible sources of error include manual coregistration of electrode locations to the head models and the lack of a tEEG specific forward model. Exact locations of the electrodes were not measured or recorded. Therefore, a position digitizer would help localization in future efforts such that channel locations need not be placed manually on the head model. Increasing the electrode density and head coverage would also help in localization, as 19 channels per recording is sparse

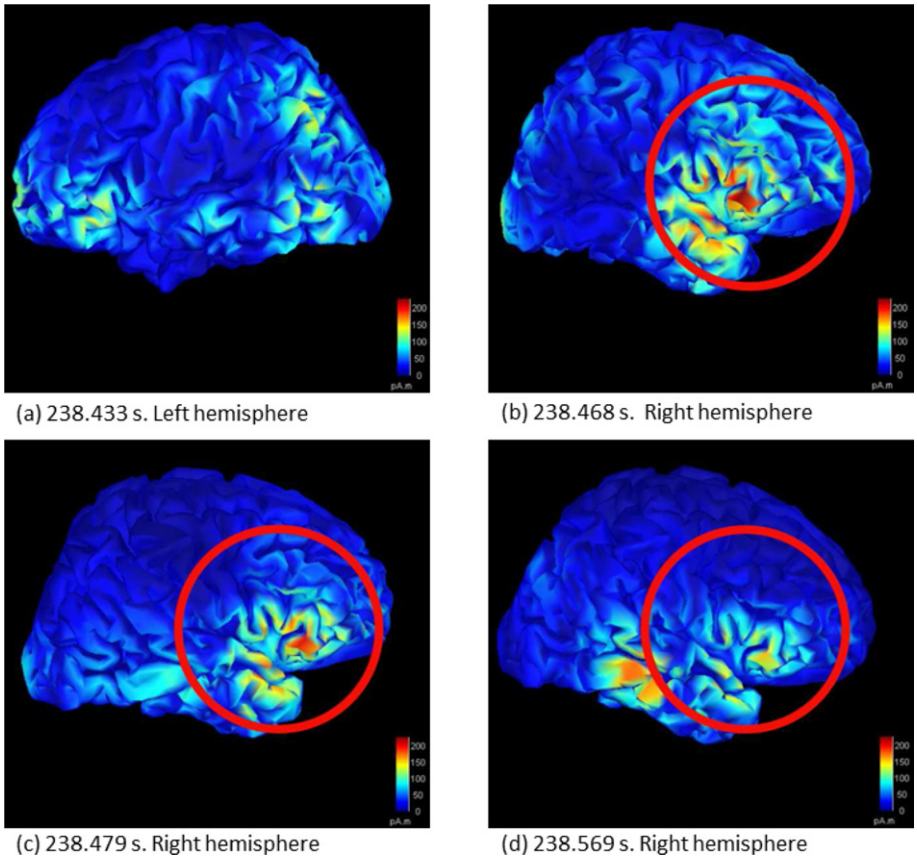


**Fig. 5.** Source localization results of HFA peaks recorded in the tEEG of patient G at approximately 238 s into recording segment. Approximately 8 min prior to a complex partial seizure. Approximate seizure onset zone is circled in red.

coverage. Song et al. [40] performed MNE and standardized low resolution brain electromagnetic tomography (sLORETA) source localization of epileptic spike activity with 32, 64, 128, and 256-channel upper head coverage and whole-head coverage montages. They found poor results with less than 64 channels and asymptotic improvement above this number. Mislocalization was found in all sampling densities using only the upper head surface, and a 256-channel montage with a 2-cm intersensor distance over the entire head, upper, and inferior surfaces produced the best results [40]. Thus, the 19-channel, upper head montage used here is a major limiting factor. Future studies should explore the relationship of head coverage and number of tEEG channels used for localization. The improved spatial resolution of the TCRE would likely lead to less required channels to achieve an accuracy obtained from conventional EEG. It is also likely that a 256-channel, whole-head coverage montage would yield more accurate and focal results than the conventional EEG of the same montage.

Moreover, the development of a tEEG forward model is crucial to future source localization studies with the TCRE. Conceptually speaking, the inverse operator fits the forward model to the recorded data, calculating the maximum likelihood distribution of activation on the model to best explain the data. Currently, the forward solution for EEG is used for tEEG localization. Thus, source localization is calculated as if the recording is EEG, and its resulting magnitude should not be received with confidence because the inverse operator is calculating this value as if the inputs are surface potentials while they are actually potential differentials estimating the Laplacian. It is difficult to say exactly how a tEEG forward model would affect the results. The effect would largely depend on the position of sources relative to the TCRE and their orientation with respect to the scalp surface (i.e., tangential or radial). Focality and magnitude of sources would likely be influenced by the model change, leaving the center location of found sources unchanged. It is the belief of the present authors that such a model would produce less spatially distributed results, improving the precision of tEEG source localization. Therefore, future development of a tEEG forward model to study its influence on resulting sources is a paramount next step in tEEG source location research. Its implementation would require the forward model to be defined with sufficient resolution to determine potential differences between distances equal to TCRE ring spacing. Then, lead field matrix values could be calculated using the nine-point method as described in Besio et al. [14].

Despite these drawbacks, localization of HFA generators in tEEG was highly correlated with SOZ/IZ diagnoses. In each patient, HFA generators were found in the SOZ/IZ, and in only one patient, G, these generators were found outside the SOZ without a strong physiological explanation. Further, the total duration of identified HFAs was very small, lasting a few hundred milliseconds each. The HFAs preceded the seizures by varying lengths from about 3 min to an hour but were not constantly present during that period and would be considered a small percentage of the total recording. Additional evidence, although limited, also suggests that HFAs in tEEG may prove to be useful biomarkers for determining underlying etiology of the epilepsy such as brain tumors and tuberous sclerosis. The traditional EEG did not show any unusual activity related to these conditions, and to our knowledge, there is no relevant literature on tumor-related HFA. However, tumors and lesions are often found in seizure-generating tissue. The characteristics of HFA in relation to these underlying symptoms should be explored. When compared with previously reported pathological HFOs [41,42] and to nonpathological, normal physiological HFA [43], the HFA reported here is much more narrowband. For example, the 320-Hz HFA shown in Fig. 4 spans a band of approximately 10 Hz from visual inspection. Previously reported HFOs, pathological and normal physiological, consist of frequency bands over 100 Hz wide. This spectral characteristic of tEEG HFA may prove to be a useful distinguishing feature for differentiating between pathological and nonpathological HFOs, which is a

major obstacle in the analytical use of HFOs in presurgical evaluation [41,44].

## 5. Conclusion

The TCRE allows for noninvasive measurement of a unique HFA biomarker found in patients with epilepsy and its subsequent localization. The HFA generators determined from tEEG appear to be highly correlated to clinically diagnosed SOZ/IZs. High-frequency biomarkers are often too difficult to detect without invasive procedures, making source localization of tEEG measurements a possible solution to narrowing the probable regions of interest before such procedures and their inherent risks are introduced to patients.

## Declaration of competing interest

Dr. Besio has received support from CREmedical Corp., which manufactures the t-Interface 20. None of the other authors has any conflict of interest to disclose.

We confirm that we have read the Journal's position on issues involved in ethical publication and affirm that this report is consistent with those guidelines.

## Acknowledgments

We thank our patients and their relatives for taking part in this research. We are thankful to Dr. Marycarmen Fernndez Gonzlez-Aragn and Dr. lvaro Moreno Avelln for their support while using the NINN video-EEG lab. We are also thankful to the technologists at NINN and RIH. Further, we would also like to thank Jay Vincelli for help with the references. This research was supported by The National Science Foundation (NSF) awards 1539068 to WB, SS, and LD and 1430833 to WB and do not reflect the views of NSF. This research was also supported by a Science Mathematics and Research for Transformation (SMART) scholarship awarded to CT. We would also like to acknowledge that Dr. Gaitanis is now the Chief of Pediatric Neurology, Tufts Floating Hospital, Boston, MA.

## References

[1] Ngugi AK, Bottomley C, Kleinschmidt I, Sander JW, Newton CR. Estimation of the burden of active and life-time epilepsy: a meta-analytic approach. Epilepsia. 2010; 51:883–90.
[2] Rosenow F, Lüders H. Presurgical evaluation of epilepsy. Brain. 2001;124:1683–700.
[3] Brodbeck V, Spinelli L, Lascano AM, Wissmeier M, Vargas MI, Vulliemoz S, et al. Electroencephalographic source imaging: a prospective study of 152 operated epileptic patients. Brain. 2011;134:2887–97.
[4] Dash GK, Radhakrishnan A, Kesavadas C, Abraham M, Sarma PS, Radhakrishnan K. An audit of the presurgical evaluation and patient selection for extratemporal resective epilepsy surgery in a resource-poor country. Seizure. 2012;21:361–6.
[5] Fisher RS, Webber WR, Lesser RP, Arroyo S, Uematsu S. High-frequency EEG activity at the start of seizures. J Clin Neurophysiol. 1992;9:441–8.
[6] Allen PJ, Fish DR, SJM Smith. Very high-frequency rhythmic activity during SEEG suppression in frontal lobe epilepsy. Electroencephalogr Clin Neurophysiol. 1992; 82:155–9.
[7] Jacobs J, LeVan P, Chander R, Hall J, Dubeau F, Gotman J. Interictal high-frequency oscillations (80–500 Hz) are an indicator of seizure onset areas independent of spikes in the human epileptic brain. Epilepsia. 2008;49:1893–907.
[8] Jacobs J, Zijlmans M, Zelmann R, Chatillon CE, Hall J, Olivier A, et al. High-frequency electroencephalographic oscillations correlate with outcome of epilepsy surgery. Ann Neurol. 2010;67:209–20.
[9] Besio WG, Martinez-Juarez IE, Makeyev O, Gaitanis JN, Blum AS, Fisher RS, et al. High-frequency oscillations recorded on the scalp of patients with epilepsy using tripolar concentric ring electrodes. IEEE J Transl Eng Heal Med. 2014;2:1–11.
[10] Worrell GA, Jerbi K, Kobayashi K, Lina JM, Zelmann R, Le Van Quyen M. Recording and analysis techniques for high-frequency oscillations. Prog Neurobiol. 2012;98: 265–78.
[11] Worrell GA, Gardner AB, Stead SM, Hu S, Goerss S, Cascino GJ, et al. High-frequency oscillations in human temporal lobe: simultaneous microwire and clinical macroelectrode recordings. Brain. 2008;131:928–37.
[12] Wu JY, Sankar R, Lerner JT, Matsumoto JH, Vinters HV, Mathern GW. Removing interictal fast ripples on electrocorticography linked with seizure freedom in children. Neurology. 2010;75:1686–94.
[13] Bragin A, Mody I, Wilson CL, Engel Jr J. Local generation of fast ripples in epileptic brain. J Neurosci. 2002;22:2012–21.
[14] Besio WG, Koka K, Aakula R, Dai W. Tri-polar concentric ring electrode development for Laplacian electroencephalography. IEEE Trans Biomed Eng. 2006;53:926–33.
[15] Koka K, Besio WG. Improvement of spatial selectivity and decrease of mutual information of tri-polar concentric ring electrodes. J Neurosci Methods. 2007;165: 216–22.
[16] Hamer HM, Morris HH, Mascha EJ, Karafa MT, Bingaman WE, Bej MD, et al. Complications of invasive video-EEG monitoring with subdural grid electrodes. Neurology. 2002;58:97–103.
[17] Van Gompel JJ, Stead SM, Giannini C, Meyer FB, Marsh WR, Fountain T, et al. Phase I trial: safety and feasibility of intracranial electroencephalography using hybrid subdural electrodes containing macro- and microelectrode arrays. Neurosurg Focus. 2008;25:E23.
[18] Shinnar S. The new ILAE classification. Epilepsia. 2010;51:715–7.
[19] ILAE. Proposal for revised clinical and electroencephalographic classification of epileptic seizures: from the Commission on Classification and Terminology of the International League Against Epilepsy. Epilepsia. 1981;22:489–501.
[20] ILAE. Proposal for revised classification of epilepsies and epileptic syndromes. Epilepsia. 1989;30:389–99.
[21] Ségonne F, Dale AM, Busa E, Glessner M, Salat D, Hahn HK, et al. A hybrid approach to the skull stripping problem in MRI. Neuroimage. 2004;22:1060–75.
[22] Fischl B, Salat DH, van der Kouwe AJW, Makris N, Ségonne F, Quinn BT, et al. Sequence-independent segmentation of magnetic resonance images. Neuroimage. 2004;23:S69–84.
[23] Sled JG, Zijdenbos AP, Evans AC. A nonparametric method for automatic correction of intensity nonuniformity in MRI data. IEEE Trans Med Imaging. 1998;17:87–97.
[24] Fischl B, Liu A, Dale AM. Automated manifold surgery: constructing geometrically accurate and topologically correct models of the human cerebral cortex. IEEE Trans Med Imaging. 2001;20:70–80.
[25] Dale AM, Fischl B, Sereno MI. Cortical surface-based analysis: I. Segmentation and surface reconstruction. Neuroimage. 1999;9:179–94.
[26] Gramfort A, Papadopoulo T, Olivi E, Clerc M. OpenMEEG: opensource software for quasistatic bioelectromagnetics. Biomed Eng Online. 2010;9:45.
[27] Gardner AB, Worrell GA, Marsh E, Dlugos D, Litt B. Human and automated detection of high-frequency oscillations in clinical intracranial EEG recordings. Clin Neurophysiol. 2007;118:1134–43.
[28] Tadel F, Baillet S, Mosher JC, Pantazis D, Leahy RM. Brainstorm: a user-friendly application for MEG/EEG analysis. Comput Intell Neurosci. 2011;2011.
[29] Fonov V, Evans AC, Botteron K, Almli CR, RC McKinstry, Collins DL, et al. Unbiased average age-appropriate atlases for pediatric studies. Neuroimage. 2011;54:313–27.
[30] Gramfort A, Luessi M, Larson E, Engemann DA, Strohmeier D, Brodbeck C, et al. MNE software for processing MEG and EEG data. Neuroimage. 2014;86:446–60.
[31] Hamalainen M. MNE software user's guide 2009 (version 2.7 ed.); 2009.
[32] Plummer C, Harvey AS, Cook M. EEG source localization in focal epilepsy: where are we now? Epilepsia. 2008;49:201–18.
[33] Wilson FN, Bayley RH. The electric field of an eccentric dipole in a homogeneous spherical conducting medium. Circulation. 1950;1:84–92.
[34] Kobayashi K, Yoshinaga H, Ohtsuka Y, Gotman J. Dipole modeling of epileptic spikes can be accurate or misleading. Epilepsia. 2005;46:397–408.
[35] Stenroos M, Hauk O. Minimum-norm cortical source estimation in layered head models is robust against skull conductivity error. Neuroimage. 2013;81:265–72.
[36] Akalin Acar Z, Makeig S. Effects of forward model errors on EEG source localization. Brain Topogr. 2013;26:378–96.
[37] Niedermeyer E, da Silva FHL. Electroencephalography: basic principles, clinical applications, and related fields. Lippincott Williams & Wilkins; 2005.
[38] LeVan P, Urrestarazu E, Gotman J. A system for automatic artifact removal in ictal scalp EEG based on independent component analysis and Bayesian classification. Clin Neurophysiol. 2006;117:912–27.
[39] Vergult A, De Clercq W, Palmini A, Vanrumste B, Dupont P, Van Huffel S, et al. Improving the interpretation of ictal scalp EEG: BSS-CCA algorithm for muscle artifact removal. Epilepsia. 2007;48:950–8.
[40] Song J, Davey C, Poulsen C, Luu P, Turovets S, Anderson E, et al. EEG source localization: sensor density and head surface coverage. J Neurosci Methods. 2015;256:9–21.
[41] Frauscher B, Bartolomei F, Kobayashi K, Cimbalnik J, vant Klooster MA, Rampp S, et al. High-frequency oscillations: the state of clinical research. Epilepsia. 2017;58: 1316–29.
[42] Zijlmans M, Jiruska P, Zelmann R, Leijten FS, Jefferys JG, Gotman J. High-frequency oscillations as a new biomarker in epilepsy. Ann Neurol. 2012;71:169–78.
[43] Kambara T, Sood S, Alqatan Z, Klingert C, Ratnam D, Hayakawa A, et al. Presurgical language mapping using event-related high-gamma activity: the Detroit procedure. Clin Neurophysiol. 2018;129:145–54.
[44] Engel J, Bragin A, Staba R, Mody I. High-frequency oscillations: what is normal and what is not? Epilepsia. 2009;50:598–604.